

Therapeutic and prophylactic roles of oleuropein in experimental acute lung injury: Modulation of tumor necrosis factor- α and nuclear factor erythroid 2-related factor 2 pathways

TİBET UĞUR KURAK¹, LEYLA BAHAR², ÇELEBİ ÇELİK³,
KANSU BÜYÜKAŞAR³, TUBA AYDIN⁴ and MEHMET OĞUZ KÖKSEL¹

¹Department of Thoracic Surgery, Faculty of Medicine, Mersin University, Mersin 33110, Türkiye;

²Department of Stem Cell and Regenerative Medicine, Graduate School of Health Sciences, Mersin University, Mersin 33110, Türkiye;

³Department of Medical Pharmacology, Faculty of Medicine, Mersin University, Mersin 33110, Türkiye;

⁴Department of Pharmacognosy, Faculty of Pharmacy, Ağrı Ibrahim Çeçen University, Ağrı 04010, Türkiye

Received March 23, 2026; Accepted May 29, 2026

DOI: 10.3892/etm.2026.13219

Abstract. In total, 10.4% of patients with acute hypoxemic respiratory failure that are treated in intensive care units develop acute respiratory distress syndrome (ARDS); this condition currently represents an incontrovertible health problem due to its high mortality rates, which have been reach ~40%. Following the rise in ARDS cases during the coronavirus disease 2019 pandemic, awareness of this disease has notably increased, emphasizing the importance of its prevention, early diagnosis and treatment. Despite numerous studies on this disease, to the best of our knowledge, no effective treatment options for ARDS have been identified outside of supportive therapies. A total of 30 female Wistar Albino rats were used to establish an ARDS model in the present study. Acute lung injury was induced in rats by administering intravenous oleic acid (OA). Intraperitoneal oleuropein (OLE) prophylaxis and therapeutic administration were then performed in model rats to investigate the prophylactic and therapeutic benefits of OLE on lung injury. The extent of lung damage after different OLE treatments was evaluated biochemically, histopathologically and immunohistochemically. Histopathological and immunohistochemical analyses revealed that OA-induced lung damage was significantly reduced in the groups treated with OLE compared with the ARDS model group. In the prophylactic OLE group, the total damage score of rat lung tissue was significantly reduced compared with that in the OA group. This was also the case for rats in the therapeutic OLE

group, but the total damage score of lung tissues in this group was slightly higher compared with that in the prophylactic group. Therefore, the present study demonstrated that OLE significantly alleviated lung damage in rats. Based on these findings, OLE may be considered a potential therapeutic agent for ARDS and therefore the findings of the present study may guide future research in this field.

Introduction

Acute respiratory distress syndrome (ARDS) is a medical condition that is characterized by non-cardiogenic pulmonary edema and acute hypoxemic respiratory failure with diffuse lung inflammation (1). ARDS was first reported by Ashbaugh *et al* (2) in 1967. Since then, numerous revisions have been made to its definition and diagnostic criteria (3). Acute lung injury (ALI) represents a milder form of ARDS that progresses through a complex and stepwise process that frequently culminates in fulminant respiratory failure and patient mortality (4). In a study reported by Bellani *et al* (5), ARDS was observed in 10.4% patients with acute hypoxemic respiratory failure in intensive care units, demonstrating a mortality rate of ~40%. Therefore, understanding of the pathophysiology of ALI and ARDS is important for their effective management and for developing potential future therapies.

ALI is characterized by pulmonary edema caused by the dysregulation of inflammation and disruption of the alveolocapillary barrier (3). A number of risk factors, such as pneumonia, thoracic trauma (pulmonary contusion), sepsis and blood transfusions, have been shown to trigger dysregulated inflammatory responses, as well as excessive leukocyte and platelet activation and increased permeability of the alveolar-capillary barrier, ultimately leading to ALI or ARDS (6). The progression of ARDS has been proposed to consist of three distinct phases: i) The acute/exudative phase; ii) the organized/proliferative phase; and iii) the late/fibrotic phase (7). The acute phase of ARDS is characterized by the presence of notable hyaline membranes that line the alveolar spaces, which frequently exhibit edemas and acute alveolar

Correspondence to: Dr Tibet Uğur Kurak, Department of Thoracic Surgery, Faculty of Medicine, Mersin University, Apartment 31, Building 1B, 2239th Street, Elmaşehir, Merkez/Karaman, Mersin 33110, Türkiye
E-mail: tibet155@gmail.com

Key words: acute lung injury, rats, oleuropein, antioxidants, oleic acid

hemorrhages (7). Concurrently, the necrosis of endothelial cells and pneumocytes is observed (7). Granulation tissue proceeds to develop within the alveolar spaces of patients with acute-phase ARDS and type II pneumocytes exhibit notable reactivity and hyperplasia toward the end of the early phase (7). These characteristics have also been shown to persist throughout the proliferative phase (7). At this stage, dense squamous metaplasia may be observed (7). As the proliferative phase progresses, granulation tissue extends into the alveolar septa, resulting in notable levels of fibrosis in the alveoli (7). During the fibrotic phase, the alveolar walls exhibit dense collagen fibrosis and hyalinization (7).

The cornerstone of current ARDS management is the identification and treatment of its underlying cause. In addition to treating its underlying causes, ARDS is clinically managed with supportive therapies, which primarily entail ventilator strategies. However, to the best of our knowledge, an effective targeted treatment for ARDS beyond supportive therapies has remained elusive (1,6).

As the incidence of ALI and ARDS has notably increased following the coronavirus disease 2019 (COVID-19) pandemic, awareness of these conditions has notably increased the importance of their prevention, early diagnosis and treatment (8). Oleuropein (OLE) is a secoiridoid compound that is extracted from unprocessed olive fruits and leaves (9) (Fig. 1). It is the predominant phenolic component found in olive leaves and has demonstrated anti-inflammatory, antioxidant and anti-apoptotic activities in multiple ischemia models; therefore, OLE has been shown to exhibit notable potential therapeutic functions (10). The present study aimed to investigate the protective and therapeutic effects of OLE in an ALI model induced by oleic acid (OA).

Materials and methods

Animals. Ethical approval for the present study was obtained from the Local Ethics Committee for Animal Experiments at Mersin University (Mersin, Turkey; approval no. 2024/25; September 27, 2024). In total, 30 adult female Wistar Albino rats (weight, 200-300 g; age, 3-4 months) obtained from the Experimental Animal Production and Research Center of the Mersin University Faculty of Medicine were included. All experimental procedures were performed in accordance with the Guidelines for the Care and Use of Laboratory Animals. During the experiment, rats were provided with standard pellet feed and tap water *ad libitum* and were housed under a 12-h light/dark cycle, 60% humidity and at a temperature of $21\pm 1^\circ\text{C}$. To induce lung injury, an OA solution was prepared by dissolving OA in 75 mg/ml ethanol and diluting it with saline. OA was purchased from Sigma-Aldrich (cat. no. O1008; Merck KGaA). An OLE solution was prepared by dissolving OLE in 100 mg/ml DMSO. To establish a model of ALI, rats were injected with 60 mg/kg OA solution through the tail vein using a 26-g syringe.

The rats were randomly divided into the following six groups (n=5/group): i) Group 1, which received intravenous (IV) administration of an ethanol control; ii) group 2, which received 60 mg/kg OA by IV administration; iii) group 3, the prophylactic group, which first received 100 mg/kg OLE by intraperitoneal (IP) injection, followed ~30 min later by IV

administration of 60 mg/kg OA; iv) group 4, the therapeutic group, which received 60 mg/kg OA by IV administration followed by 100 mg/kg OLE by IP injection ~15 min later; v) group 5, the OLE control, which received 100 mg/kg OLE via IP administration; and vi) group 6, which received DMSO administered via IP injection.

In total, 4 h after the administration of OA to rats in all treatment groups and solvent to rats in the control groups, rats were anesthetized via IP administration of 90 mg/kg ketamine and 10 mg/kg xylazine. Subsequently, 4-5 ml blood samples were taken from the inferior vena cava of rats by laparotomy. Rats were then euthanized by exsanguination under anesthesia. Lung tissues were subsequently collected and divided for tissue homogenization, histopathological and immunohistochemical analyses. Blood samples were centrifuged at $4,000 \times g$ for 10 min at room temperature and the sera were extracted and stored at -80°C for biochemical analysis.

Biochemical analysis. In serum and tissue homogenates of the collected samples, malondialdehyde (MDA), lipid peroxide (LPO), surfactant protein-D (SP-D), total antioxidant status (TAS) and total oxidant status (TOS) were analyzed biochemically. For biochemical analyses, the serum concentrations of MDA (cat. no. E0156Ra), LPO (cat. no. E0285Ra) and SP-D (cat. no. E1072Hu) were determined using ELISA kits from Shanghai Korain Biotech Co., Ltd. according to the manufacturer's protocols. The TAS (cat. no. RL0024) and TOS (cat. no. RL0017) of samples were analyzed using kits from Rel Assay Diagnostics (MEGA TIP San. Tic. Ltd. Sti.) according to the manufacturer's protocol. For tissue homogenization, 25-50 mg lung tissue was collected, 500 μl PBS was added and tissues were homogenized for 1 min. The tubes were centrifuged at $12,000 \times g$ (4°C) for 2 min, and the supernatant was collected and analyzed biochemically using the aforementioned commercial kits.

Histopathological and immunohistochemical analysis. Lung tissues were evaluated histopathologically using hematoxylin and eosin (H&E) staining. Tissue samples were fixed in 10% neutral buffered formalin at room temperature for 24 h. Following paraffin embedding, specimens were sectioned at a thickness of 4-5 μm and mounted on glass slides. Sections were deparaffinized in xylene and rehydrated through a graded ethanol series. Slides were stained with hematoxylin for 5 min at room temperature, rinsed in running tap water, differentiated and blued and then counterstained with Eosin for 2 min at room temperature ($20-25^\circ\text{C}$). After dehydration and clearing, slides were coverslipped using a permanent mounting medium. Histological examination was performed using a light microscope (Olympus BX53, Olympus Corporation, Tokyo, Japan). Histomorphometric and image analyses were conducted using Stream Basic image acquisition and analysis software version 2.4 (Olympus Corporation).

The immunoreactivity of lung tissues for TNF- α and nuclear factor erythroid 2-related factor 2 (Nrf-2) were analyzed immunohistochemically. Paraffin-embedded tissue sections (5 μm) were used for immunohistochemical analysis. Following deparaffinization and rehydration, antigen retrieval was performed in 10 mM citrate buffer (pH 6.0) by heating

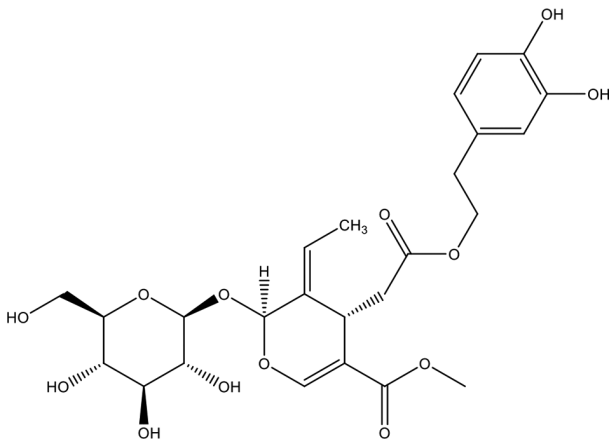


Figure 1. Chemical structure of oleuropein.

at 95-100°C for 20 min. The sections were washed three times with PBS, pH 7.4). Endogenous peroxidase activity was blocked using 3% hydrogen peroxide for 10 min, followed by blocking with a protein blocking solution (Abcam, ab64226), supplied as a ready-to-use (undiluted) reagent, for 20 min at room temperature. Sections were 1/200 diluted incubated with primary antibodies against monoclonal Anti-TNF-alpha (Abcam- cat. No. ab220210) and Polyclonal Nrf2 (Abcam, cat. no. ab137550) at 4°C overnight. Sections were incubated with HRP Polymer Quanto secondary antibody (ready-to-use; Thermo Fisher Scientific™, UltraVision™ Quanto Detection System HRP DAB, Cat. No. TL-125-QHD) for 30 min at room temperature. Immunoreactivity was visualized using a DAB chromogen system and counterstained with hematoxylin. Slides were examined using a light microscope, and images were captured and analyzed using Stream Basic software (versions 1.6-1.8, Olympus Corporation, Tokyo, Japan).

Lung tissue sections were stained with H&E and evaluated under a light microscope. Images of stained samples were captured at x20 and x40 magnification. Lung damage was assessed using a 'Total Damage score' based on the presence of interstitial edema, alveolar congestion, alveolar septa thickness, and inflammatory cell infiltration. Each parameter was rated on a scale of 0 to 3 (0: normal, 1: mild, 2: moderate, 3: severe). The total lung damage score was calculated by evaluating 6 areas for each sample and taking the arithmetic mean of the scores for these parameters. Furthermore, for the semi-quantitative analysis of immunoreactivity, signal intensity and antibody distribution were analyzed by a histologist blinded to the experimental groups of samples. An overall immunohistochemistry composite score (H-score) was generated by categorizing the staining intensity (range, 0-3) of sections across all 6 fields observed per slide using the following criteria: i) Fields with negative staining were scored 0; ii) weak staining was assigned a score of 1; iii) areas of moderate staining were scored 2; and iii) fields with strong staining intensity were assigned a score of 3. The results of semi-quantitative analyses were calculated using the formula: $H\text{-score} = \sum Pi (i + 1)$, with i indicating staining intensity and Pi representing the percentage of stained cells. The Pi -value ranged from 0-100% and each field of view received a maximum H-score between 0 and 400.

Purification of OLE from olive leaves. OLE was isolated by Dr Tuba Aydın (Department of Pharmacognosy of Ağrı Ibrahim Çeçen University (Ağrı, Türkiye)). The isolation procedure was performed as described in a previous study by Aggul *et al* (11). Olive tree (*Olea europaea*) leaves (500 g) that were collected from Yusufeli (Artvin; Turkey) in 2021 were dried, ground and powdered. Leaves were first macerated with ethanol (5 l) at room temperature for 24 h and filtered. Ethanol was removed under reduced pressure using a rotary evaporator (42°C, 90 rpm) for ~40 min. Ethyl acetate (500 ml) was then added to the concentrated ethanol extract until precipitation occurred. The precipitate was separated, and the remaining solvent was removed under reduced pressure using a rotary evaporator (35°C, 90 rpm) for ~30 min. As a result of these processes, 78 g ethanol extract was obtained (15.6% yield). The ethanol extract (10 g) was subsequently fractionated by silica gel column chromatography. Silica gel 60 (70-230 mesh, TEKKİM, Türkiye) was suspended in a dichloromethane:methanol (80:20, v/v) solvent mixture and loaded onto the column (40x3 cm, Çalışkan Lab). Fractions (40 ml) were analyzed by thin-layer chromatography and OLE-containing subfractions 7-9 (1.7 g) were combined. To isolate OLE, subfractions 7-9 were subjected to a second silica gel column chromatography under the same conditions, which improved the enrichment and recovery of OLE, resulting in a higher isolated yield. The chemical structure was determined by ¹H and ¹³C nuclear magnetic resonance spectroscopic methods. The purity of the isolated OLE was determined by High-performance liquid chromatography analysis to be 84.19%. A stock solution of oleuropein was prepared in methanol at a concentration of 500 µg/ml. Chromatographic analysis was performed using a C18 (ODS-3V) column. The mobile phase consisted of solvent A (0.1% formic acid in water) and solvent B (100% methanol) in an isocratic ratio of 60:40 (v/v). The flow rate was maintained at 1.0 ml/min, and the column oven temperature was set at 30°C. The injection volume was 10 µl. Detection was carried out using a photodiode array detector at 280 nm. The total run time was 30 min. Oleuropein concentration was determined from the corresponding peak area using an external standard calibration method. **Statistical analysis.** Statistical analysis was performed using GraphPad Prism (version 9.0; Dotmatics). The Shapiro-Wilk test was applied to assess the normality of data, and the distribution of data was normal. Data are presented as the mean and standard deviation of 5 independent experimental repeats/group. Comparisons between group means of the parameter values were analyzed via one-way ANOVA. Post hoc pairwise comparisons were performed using the Tukey test. P<0.05 was considered to indicate a statistically significant difference.

Results

H&E total damage score. Total damage scores were evaluated histopathologically in rat lung tissues using H&E staining (Fig. 2). The total damage scores of each group were compared with those of group 2 (Table I). In group 2, the lung tissue architecture was markedly disrupted compared with that in group 1; notable hemorrhagic foci were observed in the pleural and subpleural spaces. Alveolar septal thickening, widespread edema, alveolar collapse and peribronchial inflammatory-cell

Table I. Comparison of the total damage score of the oleic acid model group with other groups.

Comparison	Mean difference	Adjusted P-value	95% CI
G2 vs. G1	+1.42	<0.001	(0.75, 2.09)
G3 vs. G2	-1.03	0.002	(-1.80, -0.26)
G4 vs. G2	-0.79	0.012	(-1.47, -0.12)
G5 vs. G2	-1.33	<0.001	(-2.01, -0.66)
G6 vs. G2	-1.41	<0.001	(-2.10, -0.72)

G, group; CI, confidence interval.

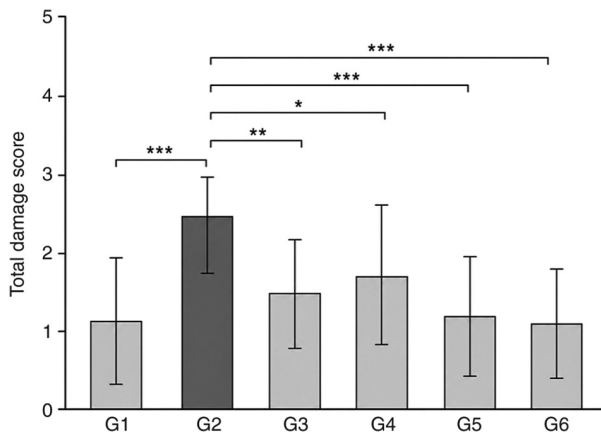


Figure 2. Intergroup comparison of total damage score, as determined by hematoxylin and eosin staining. * $P < 0.05$, ** $P < 0.01$ and *** $P < 0.001$ vs. G2, G, group.

infiltration were also observed in the lung tissue of rats in group 2. (Fig. 3) The highest total histopathological damage score of lung tissues was observed in group 2 (2.50 ± 0.88), and this increase was significantly higher compared with the scores of all other groups (Fig. 2 and Table I). In group 3, alveolar structures demonstrated improved preservation compared with those in group 2. Although hemorrhagic and edematous areas remained present in the lung tissues of group 3, the presence of these features was notably reduced compared with those in group 2. The lung tissues of rats in group 3 also demonstrated milder inflammatory-cell infiltration than in group 2 (Fig. 3). The total damage score was significantly lower in group 3 lung tissues compared with that in group 2 (mean \pm SD, 1.47 ± 0.74 ; Fig. 2; Table I). In group 4, lung damage was moderately reduced compared with the lung tissues of rats in group 2: Alveolar structures were partially preserved, hemorrhagic foci were limited and moderate inflammatory infiltration was observed (Fig. 3). The total damage score of lung tissues from rats in group 4 was significantly reduced compared with that of group 2 rats (mean \pm SD, 1.71 ± 0.86 ; Fig. 2; Table I).

TNF- α immunoreactivity. The immunohistochemical levels of TNF- α immunoreactivity were examined across experimental groups and statistically compared using H-score values (Figs. 4 and 5). Group 2 exhibited the highest level of TNF- α

expression; this increase in immunoreactivity compared with all other groups was statistically significant. Notable positive staining for TNF- α was observed in the alveolar epithelial cells, interstitial spaces and peribronchiolar regions of tissues in group 2. However, in the lung tissues of rats in group 3, TNF- α expression significantly decreased compared with that in group 2. Positive staining in group 3 was more limited to specific areas compared with the staining distribution in group 2. Furthermore, in group 4, TNF- α expression was decreased compared with that in group 2, but was markedly higher compared with TNF- α expression levels in group 3 (Fig. 5).

Nrf-2 immunoreactivity. The immunohistochemical levels of Nrf-2 immunoreactivity were examined across the experimental groups and resulting H-score values were compared (Figs. 6 and 7). In group 2, Nrf-2 expression was significantly increased as a result of the oxidative stress response induced by OA. Notable immunoreactivity was observed in the alveolar epithelium and interstitial regions of lung tissue in group 2. The mean immunoreactivity score in group 2 was significantly higher compared with that in all other experimental groups. In the lung tissues of rats in treatment group 3, Nrf-2 expression was significantly decreased compared with those in group 2. This indicated that OLE suppressed the oxidative stress response and exhibited a protective effect against lung damage. In group 4, Nrf-2 expression was decreased compared with that in group 2, but slightly higher compared with that in the prophylactic group.

Biochemical analysis. Blood samples and lung-tissue homogenates were biochemically analyzed to determine MDA, LPO and SP-D concentration in each experimental group, and TAS and TOS parameters were measured. Intergroup comparisons for all analyzed biomarkers demonstrated no significant differences (data not shown).

Discussion

ARDS is a condition that is characterized by acute hypoxemic respiratory failure and the presence of bilateral pulmonary infiltrates that cannot be explained by cardiac failure or fluid overload (3). In a study reported by Bellani *et al* (5), ARDS development was observed in 10.4% of patients in intensive care units that exhibited acute hypoxemic respiratory failure, demonstrating a mortality rate of ~40% (5). In addition to these notable mortality rates, the prevention and treatment of ARDS have become more important due to notable morbidity rates, high intensive care costs and the increasing number of ARDS cases associated with the COVID-19 pandemic (8).

Supportive therapies remain the primary approach to managing ARDS, specifically ventilator strategies (1). However, despite advances in intensive care facilities, mortality rates remain high, as there are no effective, targeted therapies for ARDS beyond supportive treatment (1). This lack of effective ARDS treatment has driven the search for targeted therapies, which has been exemplified by previous studies (1,6). The majority of these studies have focused on developing prophylactic treatments aimed at preventing the development of ARDS (1,6). Although these targeted therapies for ARDS prophylaxis appear theoretically successful, the practical

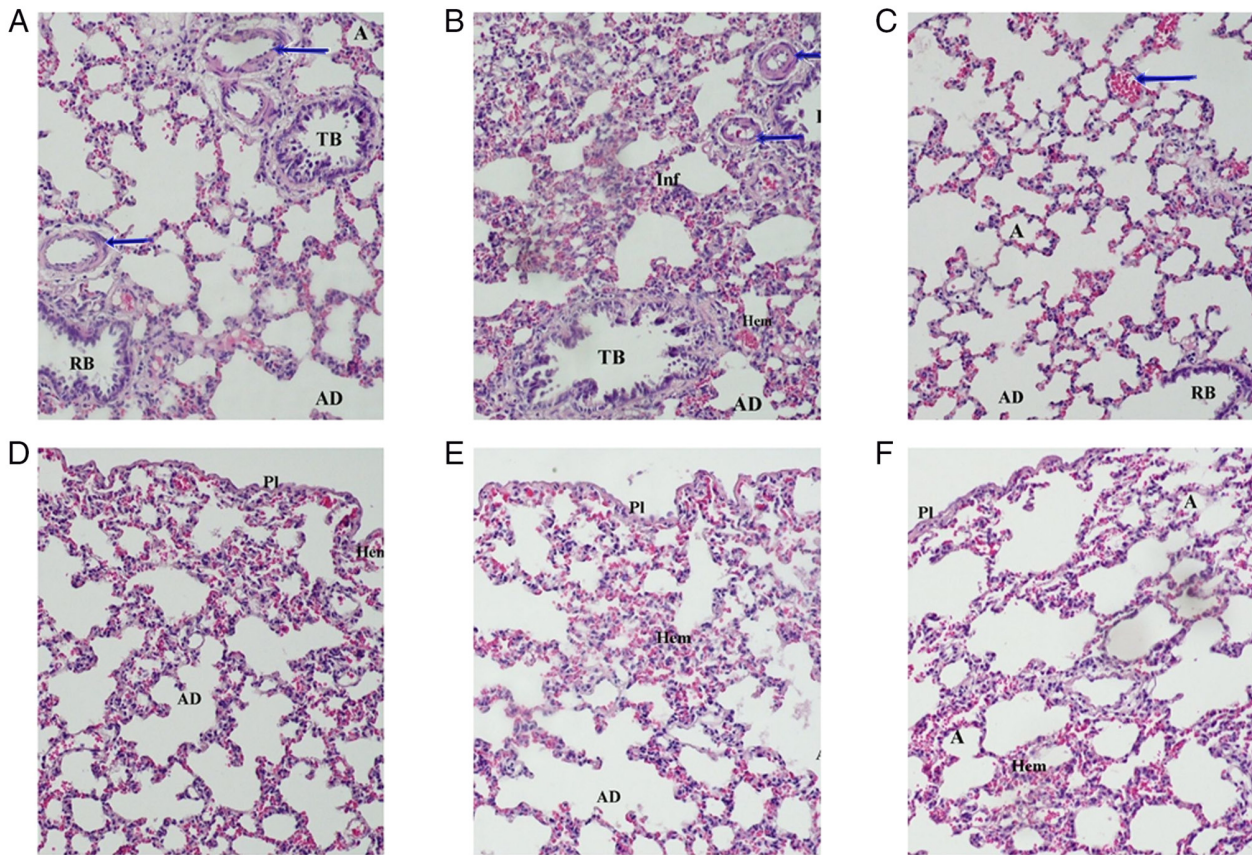


Figure 3. Histopathological examination of rat lung tissue was performed via H&E staining. Representative images of rat lung tissues stained with H&E in the (A) ethanol control, (B) OA, (C) prophylactic OLE, (D) therapeutic OLE, (E) OLE control and (F) DMSO control groups (x20 magnification). Arrows indicate arterioles. Notable hemorrhage, edema and inflammatory cell infiltration were observed in the OA group, whereas reduced damage was observed in the lung tissues of rats in the prophylactic and therapeutic OLE groups. A, alveolus; AD, alveolar duct; RB, respiratory bronchiole; TB, terminal bronchiole; PI, pleura; Hem, hemorrhage; Inf, infiltration; H&E, hematoxylin and eosin; OA, oleic acid; OLE, oleuropein.

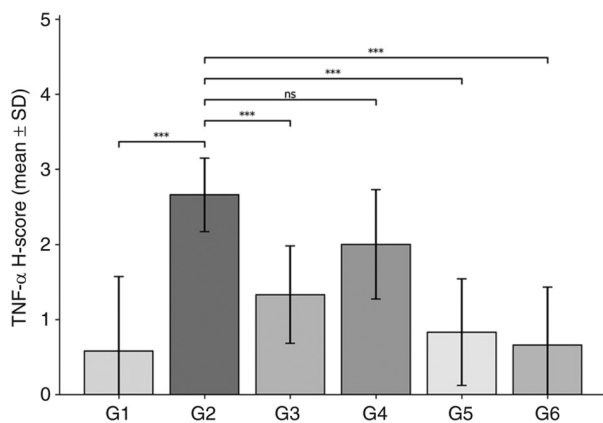


Figure 4. TNF-α H-score. ***P<0.001 vs. G2. G, group.

application of prophylactic treatments remains limited due to the acute nature of ARDS (1,6). Therefore, the present study compared two different treatments: One treatment aimed at preventing the development of ARDS and another aimed at reducing the severity of ARDS after its development.

In the present study, OA was used to establish a rat model of ARDS, as OA administration has been shown to rapidly cause ARDS-like lung damage. Histological changes in the lungs during this OA-induced damage are similar to the pathological

changes observed in the exudative phase of ARDS and manifest as edemas in the interstitial and intra-alveolar regions, intra-alveolar hemorrhages, intravascular coagulation and vascular congestion, which can be observed minutes after IV administration of OA (12). In the present study, these pathological changes were also found to be notably more prominent in the lung tissues of rats in the OA-induced ARDS model group compared with those in the other groups. In addition, the present study used OLE as a treatment to prevent and reduce the severity of lung damage. The protective effect of OLE on OA-induced lung damage was assessed by comparing the prophylactic administration of OLE, which involved OLE treatment prior to inducing lung injury with OA, with the therapeutic group, for which lung damage was induced initially with OA and followed by OLE treatment.

OLE is the predominant phenolic compound present in olive leaves and has notable anti-inflammatory, antioxidant and anti-apoptotic activities. In a previous study by Xu *et al* (10), OLE was shown to markedly ameliorate lung ischemia-reperfusion injury by reducing the activity of the toll-like receptor 4 signaling cascade in alveolar macrophages (10). Caglayan *et al* (13) demonstrated that OLE can exert anti-inflammatory effects through lipoxygenase and leukotriene B4 inhibition (13). In a study reported by Dikmen *et al* (14), OLE was administered prophylactically to rats by oral gavage for 20 days, demonstrating that OLE

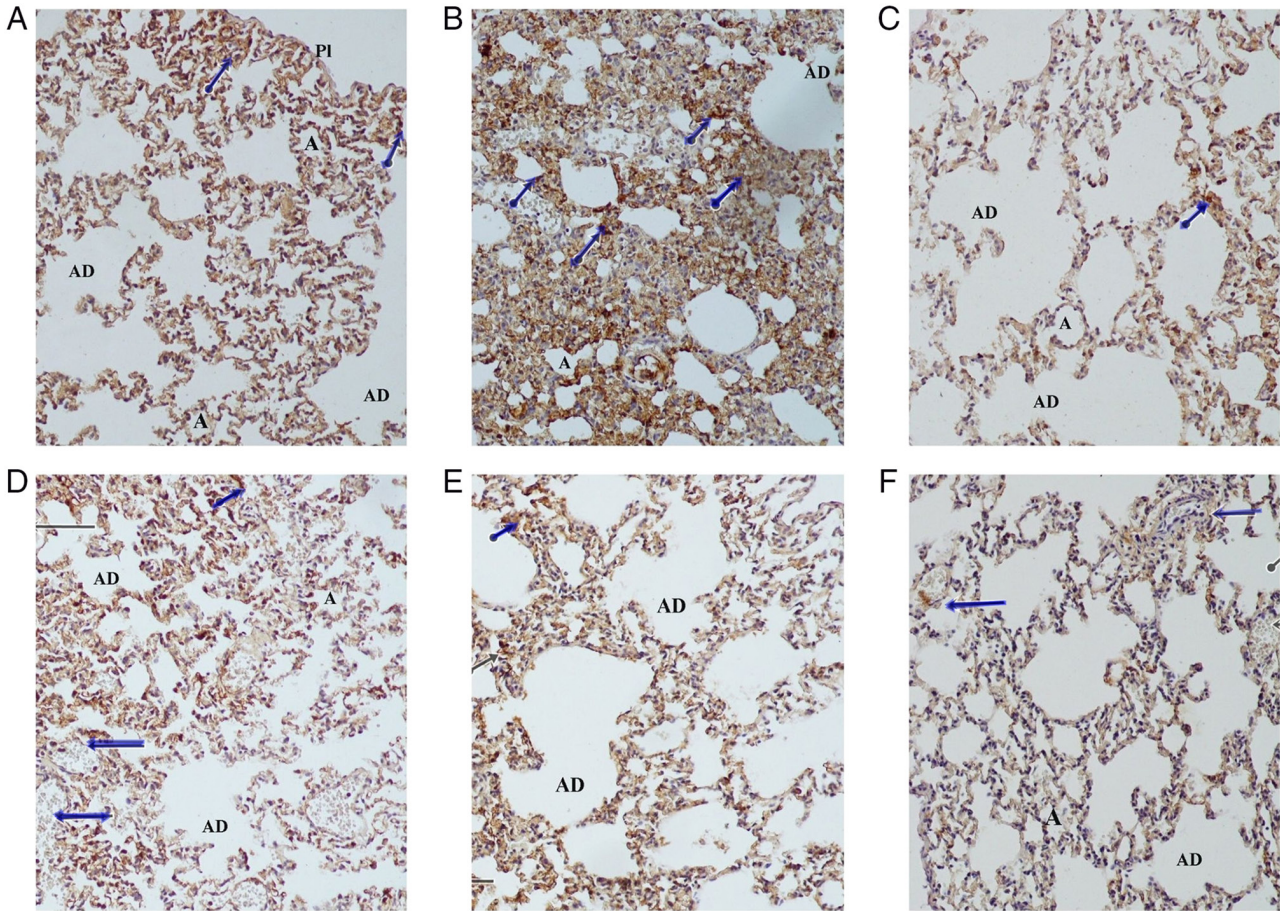


Figure 5. Immunohistochemical examination of TNF- α immunoreactivity levels in the lung tissues of acute lung injury model rats. Representative images of immunohistochemical staining for TNF- α in rat lung tissues in (A) ethanol control, (B) OA, (C) prophylactic OLE, (D) therapeutic OLE, (E) OLE control and (F) DMSO control groups (x20 magnification). Left-facing arrows indicate arterioles and shorter arrows with a circular base indicate areas of notable immunoreactivity. The OA group demonstrated the strongest immunostaining against TNF- α , whereas immunostaining notably decreased in the lung tissues of rats in the prophylactic and therapeutic OLE groups. A, alveolus; AD, alveolar duct; PI, pleura; OA, oleic acid; OLE, oleuropein.

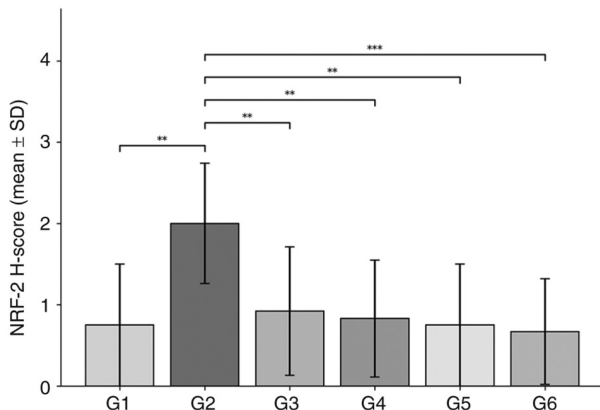


Figure 6. Nrf-2 H-score. **P<0.01 and ***P<0.001 vs. G2. G, group.

reduced lipopolysaccharide-induced ALI. Based on the aforementioned findings, a 20-day treatment period was deemed impractical for the present study, which employed an ARDS disease model; as ARDS demonstrates an acute and subtle disease onset, the present study required a study plan that established prophylactic and therapeutic treatment groups treated with a single dose of OLE. To

permit more rapid observations of treatment efficacy, OLE was administered intraperitoneally rather than orally through gavage. In the present study, a single dose of OLE (100 mg/kg) was selected for use in treatments based on previous studies that have demonstrated the biological efficacy and safety of OLE in experimental models (10,13,14). However, the absence of a dose-response analysis for OLE represents a notable limitation of the present study. As such, further studies involving multiple dose levels of OLE are required to determine the optimal therapeutic range and dose-dependent effects.

In the present study, the lung tissues of rats were examined via H&E staining; this primarily involved comparisons between the lung tissues of rats in group 2 and other experimental groups. The present study observed that the total damage score was significantly reduced in rats treated with prophylactic OLE compared with that of the model group. Compared with the model group, a significant reduction in total damage score was also observed in the group administered therapeutic OLE, but this improvement was notably milder compared with that in the prophylactic group. This difference may have been attributed to the rapid and effective lung injury-inducing effect of OA and the short duration before euthanasia in the present experimental model.

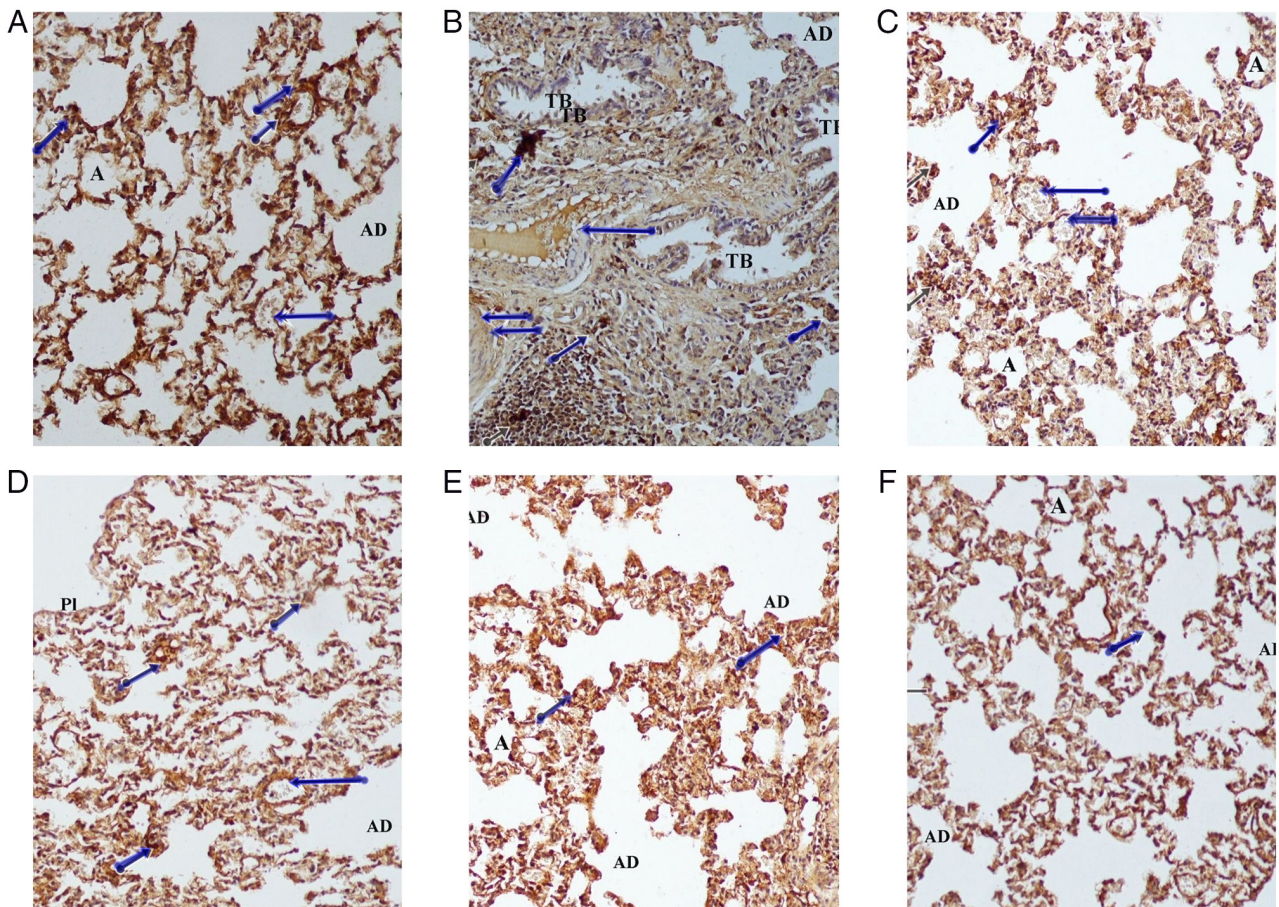


Figure 7. Immunohistochemical examination of Nrf-2 immunoreactivity levels in acute lung injury model rats. Representative images of immunohistochemical staining for Nrf-2 in rat lung tissues in the (A) ethanol control, (B) OA, (C) prophylactic OLE, (D) therapeutic OLE, (E) OLE control and (F) DMSO control groups (x20 magnification). Left-facing arrows indicate arterioles and shorter arrows with a circular base indicate areas of notable immunoreactivity. The strongest Nrf-2 immunostaining signals were observed in the lung tissues of rats in the OA group, whereas immunostaining intensity decreased in the lung tissues of rats in the prophylactic and therapeutic OLE groups. A, alveolus; AD, alveolar duct; TB, terminal bronchiole; PI, pleura; OA, oleic acid; OLE, oleuropein; Nrf-2, nuclear factor erythroid 2-related factor 2.

TNF- α was shown to serve a key role in regulating the pathophysiology of ARDS. In a number of medical conditions, such as sepsis, infection and tissue damage that causes ARDS, TNF- α has been shown to activate various signaling pathways that: i) Initiate early inflammation; ii) affect intercellular tight junction proteins; iii) increase permeability in the alveolo-capillary membrane; iv) decrease alveolar fluid clearance capacity; and v) increase neutrophil infiltration, coagulation and fibrin deposition (15-17). Therefore, TNF- α immunoreactivity levels were assessed immunohistochemically in the present study. TNF- α expression was highest in the OA-induced ARDS model group. When compared with the ARDS model group, TNF- α expression was significantly decreased in rats receiving prophylactic or therapeutic OLE, although this improvement was superior in the prophylactic OLE group.

Nrf-2 serves an important role in maintaining the balance of antioxidants and regulating various forms of cell death, such as ferroptosis and apoptosis, in the pathophysiology of ARDS (18,19). In addition, a previous study reported by Wei *et al* (20) showed that tert-butylhydroquinone, an Nrf-2 activator, exerts a protective effect on ARDS. In the present study, Nrf-2 immunoreactivity levels were evaluated immunohistochemically. The OA-induced ARDS model group was

shown to demonstrate the highest Nrf-2 expression levels across all treatment groups. Compared with the ARDS model group, Nrf-2 expression significantly decreased in the groups receiving prophylactic or therapeutic OLE; this decrease in Nrf-2 expression was notably larger in the prophylactic OLE group than the therapeutic OLE group.

The present study aimed to contribute to the development of targeted therapies for ARDS by using two different compounds derived from the same raw material, namely olive fruit and leaves (9,21). As such, lung damage was induced with OA and the efficacy of subsequent treatments with OLE was evaluated. Based on the histopathological and immunohistochemical findings of the present study, OLE demonstrated the ability to exert both protective and therapeutic effects in the targeted treatment of ARDS. Notably, the prophylactic effects of OLE administration on ARDS were found to be more potent than its therapeutic effects. This may have been due to the rapid and potent injury-inducing effects of OA after IV injection.

No statistically significant differences were observed in the biochemical parameters evaluated in the serum and lung-tissue homogenates of rats across treatment groups. Notably, the majority of the biochemical parameters evaluated in ARDS studies, such as TAS, TOS and MDA and LPO concentrations,

have been used to measure oxidant/antioxidant molecule regulation. The role of free oxygen radicals remains controversial in OA-induced models of lung injury. SP-D has been evaluated as an important indicator of alveolar epithelial integrity and lung damage (22). The aim of the present study was to analyze the levels of this molecule to determine the degree of damage in ARDS/ALI models; no significant difference ($P>0.05$) was observed in SP-D levels between groups. McGuigan *et al.* (23) demonstrated that OA-induced ARDS models did not exhibit notable free oxygen radical levels. OA-induced ARDS animal models mimic the early/exudative phase of ARDS, in which free oxygen radicals do not contribute to lung injury (23). The lack of statistically significant biochemical differences between treatment groups, despite distinct histopathological and immunohistochemical findings, may be explained by this underlying mechanism of ARDS pathophysiology. Additionally, OA has been shown to induce the rapid development of lung injury, with structural and inflammatory changes occurring within minutes of administration, whereas systemic oxidative stress markers may require a longer time to reach detectable levels (10,19). This temporal mismatch may further explain the absence of significant differences in biochemical parameters despite clear histopathological and immunohistochemical findings; the relatively short experimental duration of the present study (4 h) may have limited the detectability of systemic biochemical alterations. In addition, although the OA-induced ARDS model has been shown to reproduce key features of early-phase ARDS, this model does not fully reflect the complex and heterogeneous nature of this disease in humans (12). Therefore, the findings of the present study should be interpreted as preclinical evidence; further studies, including dose-optimization studies, pharmacokinetic analyses and clinical trials, are required before clinical application of OLE can be considered.

In conclusion, additional studies are required to develop targeted therapies for ARDS. The present study demonstrated that OLE exhibited notable potential for both protective and therapeutic effects on ARDS. The present study, alongside similar future studies, will further elucidate potential targeted therapeutic agents for ARDS and therefore guide more comprehensive research in the future.

Acknowledgements

Not applicable.

Funding

The present study was funded by the Scientific Research Project Unit of Mersin University Rectorate (grant no. 2025-TP3-5282).

Availability of data and materials

The data generated in the present study may be requested from the corresponding author.

Authors' contributions

TUK, KB and MOK were responsible for the experimental design and conceptualization of the study. TUK, KB, TA and

MOK performed literature searches. TUK, LB, ÇÇ, KB, TA and MOK were responsible for performing the animal experiments. TUK and LB contributed towards data collection and processing. TUK, LB and MOK confirm the authenticity of all the raw data. TUK, LB, ÇÇ and KB were responsible for the analysis and interpretation of results. TUK, LB, TA and MOK wrote the original draft of the manuscript. All authors read and approved the final version of the manuscript.

Ethics approval and consent to participate

Ethical approval for the present study was obtained from the Local Ethics Committee for Animal Experiments at Mersin University (Mersin, Türkiye; approval no. 2024/25; dated September 27, 2024).

Patient consent for publication

Not applicable.

Competing interests

The authors declare that they have no competing interests.

References

- Gorman EA, O'Kane CM and McAuley DF: Acute respiratory distress syndrome in adults: Diagnosis, outcomes, long-term sequelae, and management. *Lancet* 400: 1157-1170, 2022.
- Ashbaugh DG, Bigelow DB, Petty TL and Levine BE: Acute respiratory distress in adults. *Lancet* 2: 319-323, 1967.
- ARDS Definition Task Force; Ranieri VM, Rubenfeld GD, Thompson BT, Ferguson ND, Caldwell E, Fan E, Camporota L and Slutsky AS: Acute respiratory distress syndrome: The Berlin Definition. *JAMA* 307: 2526-2533, 2012.
- Butt Y, Kurdowska A and Allen TC: Acute lung injury: A clinical and molecular review. *Arch Pathol Lab Med* 140: 345-350, 2016.
- Bellani G, Laffey JG, Pham T, Fan E, Brochard L, Esteban A, Gattinoni L, van Haren F, Larsson A, McAuley DF, *et al.*: Epidemiology, patterns of care, and mortality for patients with acute respiratory distress syndrome in intensive care units in 50 countries. *JAMA* 315: 788-800, 2016.
- Mokrá D: Acute lung injury - from pathophysiology to treatment. *Physiol Res* 69 (Suppl 3): S353-S366, 2020.
- Unruh HW: Katzenstein and Askin's surgical pathology of non-neoplastic lung disease. *Can J Surg* 40: 394, 1997.
- Hussain M, Khurram Syed S, Fatima M, Shaikat S, Saadullah M, Alqahtani AM, Alqahtani T, Bin Emran T, Alamri AH, Barkat MQ and Wu X: Acute respiratory distress Syndrome and COVID-19: A literature review. *J Inflamm Res* 14, 7225-7242, 2021.
- Ahamad J, Toufeeq I, Khan MA, Ameen MSM, Anwer ET, Uthirapathy S, Mir SR and Ahmad J: Oleuropein: A natural antioxidant molecule in the treatment of metabolic syndrome. *Phytother Res* 33: 3112-3128, 2019.
- Xu Z, Sun X, Ding B, Zi M and Ma Y: Oleuropein ameliorated lung ischemia-reperfusion injury by inhibiting TLR4 signaling cascade in alveolar macrophages. *Transpl Immunol* 74: 101664, 2022.
- Aggul AG, Gulaboglu M, Cetin M, Ozakar E, Ozakar RS and Aydin T: Effects of emulsion formulations of oleuropein isolated from ethanol extract of olive leaf in diabetic rats. *An Acad Bras Cienc* 92: e20190810, 2020.
- Dickey BF, Thrall RS, McCormick JR and Ward PA: Oleic-acid-induced lung injury in the rat. Failure of indomethacin treatment or complement depletion to ablate lung injury. *Am J Pathol* 103: 376-383, 1981.
- Caglayan K, Güngör B, Cinar H, Avci B, Gur S and Arslan N: Effects of oleuropein on serum inflammatory cytokines and histopathological changes in rats with pancreatitis. *Adv Clin Exp Med* 24: 213-218, 2015.

14. Dikmen N, Cellat M, Etyemez M, İşler CT, Uyar A, Aydın T and Güvenç M: Ameliorative effects of oleuropein on lipopolysaccharide-induced acute lung injury model in rats. *Inflammation* 44: 2246-2259, 2021.
15. Huang Q, Le Y, Li S and Bian Y: Signaling pathways and potential therapeutic targets in acute respiratory distress syndrome (ARDS). *Respir Res* 25: 30, 2024.
16. Mazzon E and Cuzzocrea S: Role of TNF-alpha in lung tight junction alteration in mouse model of acute lung inflammation. *Respir Res* 8: 75, 2007.
17. Patel BV, Wilson MR, O'Dea KP and Takata M: TNF-induced death signaling triggers alveolar epithelial dysfunction in acute lung injury. *J Immunol* 190: 4274-4282, 2013.
18. Liu Q, Gao Y and Ci X: Role of Nrf2 and its activators in respiratory diseases. *Oxid Med Cell Longev* 2019: 7090534, 2019.
19. Deng J, Li N, Hao L, Li S, Aiyu N, Zhang J and Hu X: Transcription factor NF-E2-related factor 2 plays a critical role in acute lung injury/acute respiratory distress syndrome (ALI/ARDS) by regulating ferroptosis. *PeerJ* 12: e17692, 2024.
20. Wei J, Chen G, Shi X, Zhou H, Liu M, Chen Y, Feng D, Zhang P, Wu L and Lv X: Nrf2 activation protects against intratracheal LPS induced mouse/murine acute respiratory distress syndrome by regulating macrophage polarization. *Biochem Biophys Res Commun* 500: 790-796, 2018.
21. Lopez S, Bermudez B, Montserrat-de la Paz S, Jaramillo S, Varela LM, Ortega-Gomez A, Abia R and Muriana FJ: Membrane composition and dynamics: A target of bioactive virgin olive oil constituents. *Biochim Biophys Acta* 1838: 1638-1656, 2014.
22. Peukert K, Seeliger B, Fox M, Feuerborn C, Sauer A, Schuss P, Schneider M, David S, Welte T, Putensen C, *et al*: SP-D serum levels reveal distinct epithelial damage in direct human ARDS. *J Clin Med* 10: 737, 2021.
23. McGuigan RM, Mullenix P, Norlund LL, Ward D, Walts M and Azarow K: Acute lung injury using oleic acid in the laboratory rat: Establishment of a working model and evidence against free radicals in the acute phase. *Curr Surg* 60: 412-417, 2003.



Copyright © 2026 Kurak et al. This work is licensed under a Creative Commons Attribution-NonCommercial-NoDerivatives 4.0 International (CC BY-NC-ND 4.0) License.